Journal of Catalysis 283 (2011) 119–123

Contents lists available at SciVerse ScienceDirect

Journal of Catalysis

journal homepage: www.elsevier.com/locate/jcat

In situ XPS study of the adsorption and reactions of NO and O_2 on gold nanoparticles deposited on TiO_2 and SiO_2

Tirma Herranz [a,1], Xingyi Deng [a,2], Andreu Cabot [a,3], Zhi Liu [b], Miquel Salmeron [a,c,*]

[a] Materials Sciences Division, Lawrence Berkeley National Laboratory, Berkeley, CA, USA
[b] Advance Light Source, Lawrence Berkeley National Laboratory, Berkeley, CA, USA
[c] Materials Science and Engineering Department, University of California, Berkeley, CA, USA

ARTICLE INFO

Article history:
Received 17 March 2011
Revised 13 June 2011
Accepted 25 June 2011
Available online 9 September 2011

Keywords:
Gold
Titanium oxide
Ambient pressure photoelectron spectroscopy
In situ characterization
Band bending
Model catalysts
Nitric oxide

ABSTRACT

Ambient pressure photoelectron spectroscopy (APPES) has been used to study the adsorption of nitric oxide (NO) and molecular oxygen (O_2) over gold-based model catalysts consisting of mono-dispersed gold nanoparticles with different diameters (2–5 nm) and oxide supports (including polycrystalline silica and titania thin films). APPES is an in situ technique that makes possible to monitor via XPS chemical changes occurring on the catalyst surface and to identify adsorbed species under reaction conditions. In our experiments, no changes were observed on the Au/SiO_2 samples during exposure to 0.5 Torr of NO, while adsorbed NO and several N-containing species were detected on Au/TiO_2 model catalysts under the same conditions. In addition, shifts in the Ti 3p and O 1s peaks in TiO_2 were observed relative to the Au 4f peak. Similar behavior, although to a lesser extent, was observed on Au/TiO_2 samples when O_2 was used. In both cases, the shifts of the Ti 3p and O 1s peaks could be attributed to band bending effects on the TiO_2 substrate caused by chemisorption of the gases.

1. Introduction

Dispersed gold nanoparticles on oxides display high catalytic activity in a variety of reactions at room temperature [1–3]. Bulk gold, on the other hand, is inert in chemical reactions [4]. After the initial discovery of the enhanced activity of Au nanoparticles, an increasing number of reports dealing with many different reactions have followed. In order to understand the molecular level structure and composition of the catalysts under reaction conditions, it is imperative that in situ characterization techniques are utilized [5,6].

The CO oxidation with NO is an important reaction in catalytic converters at the exhaust of automobile vehicles. Currently, the traditional catalysts are based on Pt and Rh metals, with Rh being the most active metal within the typical temperature range of automobile exhaust gases [7]. The reduction of NO_x by CO at low temperature (252–369 K) over Au powder was first reported in 1975 [8]. Ueda and Haruta first reported CO oxidation by NO over supported Au catalysts [9] prepared by deposition–precipitation, with mean particle sizes between 3 and 5 nm. Although few Au-based catalysts have been used as vehicle exhaust catalysts until now, a catalyst developed by the Anglo-American Research Laboratories of South Africa has been shown to have good activity in the NO_x reduction reaction and in CO/hydrocarbon oxidation under simulated diesel engine conditions (7.5% O_2) [10].

Most of the gold-based catalysts tested for oxidation reactions have been supported on transition metal oxides where the support can play an important role [11]. In the case of CO oxidation by NO, the published literature is less extensive. Using Au nanoparticles inside meso and microporous materials (with broad particle size distribution, around 2–8 nm), Akolekar et al. [12] studied the adsorption of CO and NO with infrared spectroscopy, finding various CO and NO complexes depending on particle size, loading, catalyst structure, temperature, and pressure. The nature of the NO_x species and their concentration were influenced by the host structure (mesoporous or microporous materials). Also, the FTIR results showed that NO_x and CO were found in some Au-free supports.

The first step in the CO + NO reaction is the adsorption of the reactants. There are few references in the literature dealing with NO adsorption over Au/TiO_2. On Au(100) single crystal surfaces, the adsorption of NO lifts the hexagonal reconstruction, desorbing between 170 and 230 K [13]. On Au(111), NO desorbs at even

* Corresponding author at: Materials Science and Engineering Department, University of California, Berkeley, CA, USA.
E-mail addresses: mbsalmeron@lbl.gov, salmeron@stm.lbl.gov (M. Salmeron).
[1] Present address: Instituto de Catálisis y Petroleoquímica, CSIC, C/ Marie Curie, 2, 28049 Madrid, Spain.
[2] Present address: National Energy Technology Laboratory, Pittsburgh, PA, USA.
[3] Present address: Catalonia Institute for Energy Research, Barcelona, Spain.

0021-9517/$ - see front matter © 2011 Elsevier Inc. All rights reserved.
doi:10.1016/j.jcat.2011.06.022

lower temperature (95 K) [14]. In open surfaces, like Au(3 1 0), the desorption maximum for NO occurs at about 120 K while N_2O, formed by NO decomposition on the Au surface, desorbs at 150 K [15]. These previous results indicate that, while NO adsorbs and forms dissociation products on Au surfaces, under our room temperature conditions and NO pressures of 0.5 Torr, the steady state concentration of surface species should be completely negligible.

Several papers in the literature report studies of the interaction of NO with TiO_2 using infrared spectroscopy. Ramis and co-workers studied the adsorption of NO and NO_2 on TiO_2. They identified the presence of chemisorbed NO (nitrosyl groups) and N_2O (from the reaction with Ti^{3+}). Nitrites and nitrates were also observed after a long exposure time [16]. Hadjiivanov and Knozinger exposed TiO_2 degussa P-25 to NO and studied the species formed by FTIR [17]. They found nitrates (1650–1550 and 1240–1220 cm^{-1}), NO^- (1170 cm^{-1}) and $N_2O_2^{2-}$ (1335 cm^{-1}). When exposed to a mixture of O_2 and NO, a strong increase of nitrate related bands was observed, together with the formation of NO^+ (2206 cm^{-1}). In addition, species assigned to nitrocomplexes (1520 and 1284 cm^{-1}) were found. A band at 1950–1800 cm^{-1} was attributed to surface nitrosyls. NO adsorption over TiO_2 was also studied by FTIR by Wu and Chen [18] who found mainly nitrate and nitrite related absorption bands. Li and co-workers [19] also reported the formation of nitrates when studying NO and NO–O_2 co-adsorption over Pt/TiO_2 catalysts. NO initially adsorbs on Pt sites as linear NO species, which are further oxidized and migrate to the TiO_2 support to form various surface nitrates. On TiO_2 at room temperature, the authors observed various bands assigned to nitrates with a lesser intensity compared with the platinum loaded sample, demonstrating the catalytic effect of Pt in NO oxidation.

Debeila and co-workers studied the interaction of NO with Au/TiO_2 at room temperature. Adsorption of NO was dominated by the formation of dinitrosyl complexes, with bands at 1824 cm^{-1}. Au-NO species were also detected, with a band at 1796 cm^{-1}. Bands at 2239 and 2202 cm^{-1} corresponding to adsorbed N_2O were also identified [20]. When the CO covered surface was exposed to NO, the carbon monoxide was displaced and the formation of dinitrosyls enhanced [21].

In our studies, we used ambient pressure photoelectron spectroscopy (APPES) to characterize the adsorption of nitric oxide and molecular oxygen (for reference) over mono-dispersed gold nanoparticles supported on polycrystalline nanoporous titanium dioxide and silicon oxide. The XPS data obtained with this technique provide spectroscopic information about chemical states of the sample and the adsorbed species under the reaction conditions [22].

2. Experimental

2.1. Sample preparation

The preparation of the gold nanoparticles was described in a previous report [23]. Briefly, colloidal nanoparticles with sizes in the range 2 and 5.5 nm were synthesized by the reduction of gold (III) chloride hydrate (99.999%) with tetrabutyl ammonium borohydride (TBAB, 98%) in the presence of didodecyldimethylammonium bromide (DDAB, 98%) and dodecylamine (99%), as previously described by Jana et al. [24]. In a typical synthesis, 0.1 mmol of $HAuCl_4$ were dissolved in 10 ml of a 0.1 M DDAB solution in toluene. Next, 1 mmol of dodecylamine was added to the solution and dissolved by sonication. Finally, a solution of 0.3 mmol TBAB dissolved in 2 ml of 0.1 M DDAB in toluene was rapidly injected into the gold chloride solution under vigorous stirring in a similar way as in Refs. [25,26]. After reaction, gold nanoparticles of 2–3 nm diameters were obtained. Larger particles, up to 5 nm, were obtained by seeded growth from this initial sample. After synthesis, a 0.5 mmol hexadecanethiol solution was added to prevent aggregation. The mean size and distribution of the gold nanoparticles have been measured using high resolution transmission electron microscopy, and in all cases, the width of the size distribution curves was less than 10%, as described in Ref. [23].

For spectroscopy studies, the gold nanoparticles were deposited on flat substrates using the Langmuir–Blodgett (LB) method [27,28]. The substrates were either SiO_2/Si wafers (native oxide layer over a silicon wafer) or nanoporous TiO_2 films over a Si wafer [29,30]. Before the spectroscopic measurements, the samples were characterized by scanning electron microscopy (Zeiss Gemini Ultra-55 Analytical Scanning Electron Microscope) and laboratory-based XPS (PHI 5400). To remove the thiols from the Au nanoparticles, the samples were plasma cleaned in UV/ozone for 60 min. Micrographs of the samples before and after cleaning can be found in Ref. [23] showing that there is little agglomeration of the nanoparticles after removing the protective alkylthiol molecules.

2.2. In situ XPS experiments

All APPES measurements were carried out at the beam line 9.3.2 of the Berkeley Advanced Light Source using a photoemission spectrometer that is capable of operating at pressures of up to 5 Torr [31,32]. To ensure that the same depth is being probed in all experiments, the photon energies were selected to ensure the same photoelectron kinetic energy of 300 eV in all spectral regions. So we used photons of energy 400 eV for the Au 4f, 600 eV for C 1s, 720 eV for N 1s, and 850 eV for O 1s. After data acquisition of each spectral region, the Ti 3p peak was also recorded using the same photon energy. The area of each spectrum was normalized to the integrated intensity of the corresponding Ti 3p to correct for the intensity loss due to the scattering of gas phase molecules at high pressures.

The data analysis involved spectra normalization, Shirley background subtraction, and curve-fitting with Gaussian–Lorentzian functions. The Au 4f regions were fitted by doublets with fixed spectroscopic parameters, such as spin-orbital separation (3.67 eV) and $4f_{5/2}$:$4f_{7/2}$ branching ratio of 0.75, but with independent and variable full width half maximum (fwhm), positions and intensities as optimized by the fitting program. The O and N 1s regions were fitted by independent peaks with all parameters variable and optimized by the program.

As we have shown recently [33], the binding energy of the gold nanoparticles on TiO_2 remains fixed under a variety of conditions of pressure and temperature, similar to the ones used in the present study. For that reason, the energy scales in the XPS curves were all referenced to the BE of the Au $4f_{7/2}$, which was set at 84.0 eV, the same value as for metallic gold. Only under sufficiently high pressure of oxidizing gases or under X-ray or electron irradiation does Au become oxidized and a new Au $4f_{7/2}$ peak appears at higher binding energy, a process that can be easily detected [34].

3. Results and discussion

XP spectra of mono-dispersed Au nanoparticles (4 nm) supported on the nanoporous TiO_2 thin films in the presence of NO at pressures in the Torr range at room temperature are displayed in Fig. 1. In all cases, the samples were first heated in vacuum at 110 °C to remove weakly bound species prior to introduction of NO. When NO was introduced into the system, the peaks broadened with the increasing NO pressure, from 0.99 eV FWHM in UHV to 1.24 eV under 470 mTorr of NO (Fig. 1a).

Two peaks were observed in the O 1s region in UHV, which can be assigned to the lattice oxygen in TiO_2 at 531.0 eV, and surface

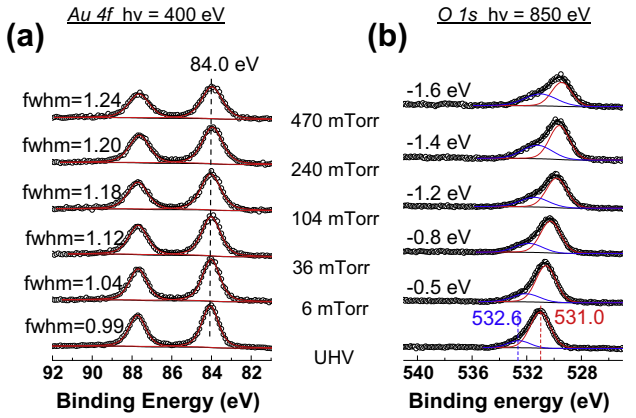

Fig. 1. (a) Au 4f XPS spectra of 4-nm mono-dispersed Au nanoparticles supported on nanoporous TiO_2 in UHV and under various pressures of NO. (b) Corresponding O 1s XPS spectra. The binding energy scale was calibrated using the Au $4f_{7/2}$ peak (84.0 eV). All spectra were taken at room temperature.

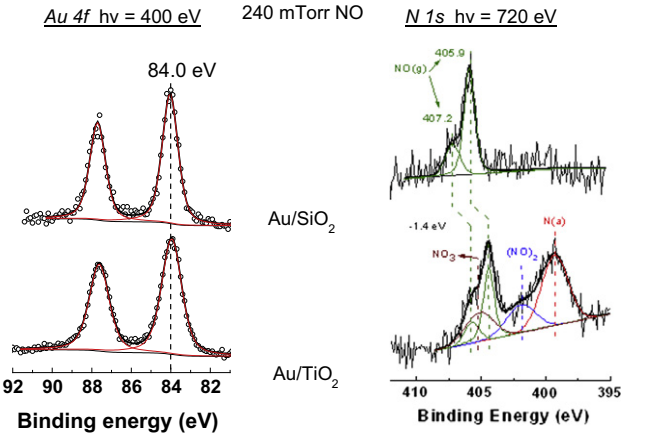

Fig. 2. Au 4f and N 1s XPS spectra of 4-nm Au nanoparticles deposited on TiO_2 and SiO_2 thin films in the presence of 240 mTorr NO.

hydroxyl groups at 532.6 (Fig. 1b). The hydroxyl groups originate from background water dissociating at the oxide surface [35]. When 6 mTorr of NO were introduced into the chamber, the two O 1s peaks shifted by −0.5 eV, and continued shifting by larger values as more NO was introduced. At 470 mTorr, the O 1s peak had shifted −1.6 eV. We also observed an increase in intensity and fwhm of the component at 532.6 eV when the pressure of NO was 470 mTorr, potentially implying new oxygen containing species on the surface, as discussed below.

The binding energy shifts in the O 1s region can be attributed to band bending in the TiO_2, as discussed in a previous work [33]. Nowotny and co-workers studied the effect of oxygen exposure on polycrystalline undoped TiO_2 films measuring the changes in the work function [36]. They found that exposure to molecular oxygen at ambient pressure increased the work function reversibly by 0.7 eV due to the adsorption of O_2 species, which according to the authors became O_2^-, as indicated in Eq. (1):

$$O_2 + Ti^{3+} \rightarrow Ti^{4+} + O_2^- \quad (1)$$

$$2NO + 2Ti^{3+} \rightarrow 2Ti^{4+} + O_2^- + N_2O \quad (2)$$

The charged O_2^- species cause the band bending and the concomitant change in work function. Increases in the work function of TiO_2 (0.4 eV) due to NO adsorption have also been observed in UHV studies after exposure to 10^{-7} Torr [37].

In order to check whether the observed peak shifts and broadening occur also when using oxygen, we dosed O_2 into the chamber. We found that the O 1s peaks also shifted to lower binding energy but less than in the case of NO. The shift was −0.7 eV for Au/TiO_2 samples with diameters of 2, 4, and 5 nm under 500 mTorr O_2. In the case of NO, due to its stronger oxidizing character, it can be easily dissociated on TiO_2. When it is adsorbed on Ti^{3+}, it can form N_2O and donate atomic oxygen through the process described in the equations above. Also, it can be oxidized on the surface of stoiquiometric TiO_2 to form NO^+ and nitrate. Therefore, it is likely that the change in work function of the TiO_2 substrate could be higher in that case.

In Fig. 2, we show the Au 4f and N 1s core level spectra of 4-nm nanoparticles supported on TiO_2 and on SiO_2 thin films in the presence of 240 mTorr of NO. On SiO_2, only the gas phase peaks from NO are visible at 405.9 and 407.2 eV. The origin of these two components has been described previously by Hosaka and co-workers [38]. A similar assignation was reported recently by Shimada et al. using the same instrumental setup as in this work. On TiO_2, however, several peaks due to adsorbed N species are visible. By reference to published literature values, we assign these species to atomic N (399.3 eV) [40] and NO_3 (405.1 eV) [41]. The peak at 401.9 eV was tentatively assigned to NO dimers or dinitrosyls species, R–$(NO)_2$, intermediates of N_2O formation from NO. Those species were described by Debeila and co-workers when exposing Au/TiO_2 samples to NO at room temperature [20]. Nart and Friend [42] found also the same mechanism when dosing NO to oxidized Mo(1 1 0) and Ertl and co-workers when adsorbing NO over MoS_2 [43]. We observe the gas phase peaks now shifted by −1.4 eV relative to the Au/SiO_2 sample. The shift reflects again the change in work function of the TiO_2 due to band bending.

The different NO chemisorption behavior of Au on the two substrates suggest that NO is chemisorbed on the TiO_2 support only. This is confirmed by the observation exposing the bare TiO_2 support to 240 mTorr of nitric oxide, i.e., the same conditions used for the Au/TiO_2 samples; the obtained N 1s spectrum is identical to that on Au/TiO_2, as shown in Fig. 3.

The reversibility of the binding energy changes due to the band bending was tested by desorbing the N-containing species, as shown in Fig. 4. The spectra at the bottom (a) are obtained after exposing the 4 nm Au/TiO_2 sample to 470 mTorr of NO. After evacuating the NO gas, the N 1s peaks shifted by 0.4 eV to higher binding energy, (middle spectra b). Removal of the gas phase decreased the intensity of the dinitrosyls and NO_3 adsorbed species. Heating

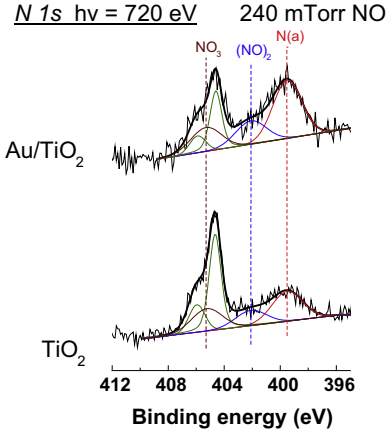

Fig. 3. N 1s XPS spectra of the bare TiO_2 thin film and that with deposited 4-nm Au nanoparticles in the presence of 240 mTorr NO. All spectra were taken at room temperature.

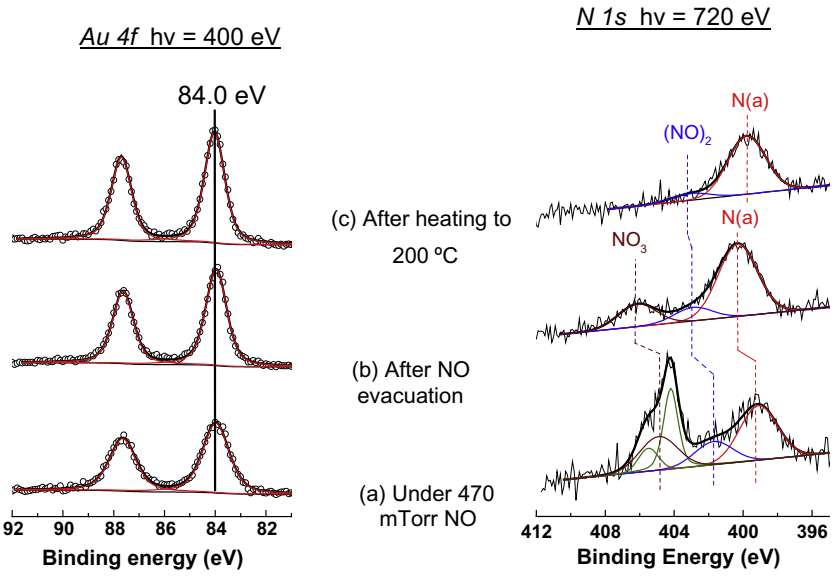

Fig. 4. Au 4f and N 1s XPS spectra of 4 nm Au over TiO_2 (a) under 470 mTorr NO at room temperature, (b) after evacuating NO and (c) after heating at 200 °C. All spectra were taken at room temperature.

Table 1
The full width at half maximum (fwhm) of Au 4f peaks in UHV and in NO.

	2 nm fwhm (eV)	4 nm fwhm (eV)	5 nm fwhm (eV)
UHV	0.94	0.99	0.94
6 mTorr NO	1.27	1.04	0.96
36 mTorr NO	1.85	1.12	1.05
105 mTorr NO	2.11	1.18	1.04
240 mTorr NO	2.17	1.20	1.01
470 mTorr NO	2.18	1.24	1.07

the sample to 200 °C in vacuum (top spectra, c) shifted the N 1s core level and caused the desorption of NO_3 and most of the dinitrosyls species. These results indicate that the adsorbed species containing oxygen and nitrogen are mostly responsible for the band bending effect, while atomic nitrogen has a minor effect.

We also studied particle size effects by measuring changes in the Au 4f peaks of nanoparticles of 2 nm, 4 nm, and 5 nm diameter. As the NO pressure increased the peaks broadened as summarized in Table 1. Interestingly in UHV, all particles had Au 4f peaks with similar fwhm (0.94–0.99 eV), regardless of size. The 2-nm sample, however, exhibited the larger change in fwhm, increasing from 0.94 to 2.18 eV when the pressure increased from ultra-high vacuum to 470 mTorr. Substantially smaller increases were observed, however, for the 4 and 5 nm particles in the same pressure range. The changes are reversible upon desorption of the NO and its dissociation products as shown in Fig. 4. It is not clear what is the mechanism driving this broadening. As we have shown, NO adsorbs only on the TiO_2 support and not on the Au particles (Fig. 3). Maybe the NO adsorbs on support sites near the Au edges of the nanoparticles, which are proportionally more abundant in small particles, modifying their binding energy. Clearly, additional experiments are needed to understand this potentially significant result. In situ high resolution imaging by scanning probe or transmission electron microscopy could provide an answer.

4. Conclusions

NO was adsorbed on model Au/TiO_2 and Au/SiO_2 catalysts prepared using mono-dispersed gold nanoparticles. Ambient pressure photoelectron spectroscopy experiments revealed that NO and O_2 adsorb only on the TiO_2 support (within the XPS sensitivity limit of ~1% of a monolayer) and gives rise to various N-containing species. Band bending effects caused by the adsorption of NO and O_2 on the TiO_2 substrate resulted in binding energy shifts of the Ti 3p, O 1s, and N 1s peaks.

Interesting changes in the width of the Au 4f core level peaks were observed that depend on particle size. Understanding the origin of this size dependent broadening may yield clues to the enhanced catalytic activity of small Au nanoparticles in CO oxidation reactions.

Acknowledgments

This work was supported by the Director, Office of Science, Office of Basic Energy Sciences, Chemical Sciences, Geosciences, and Biosciences Division, under the Department of Energy Contract No. DE-AC02-05CH11231. T.H. acknowledges the Ramon Areces foundation from Spain for financial support.

References

[1] M. Valden, X. Lai, D.W. Goodman, Science 281 (1998) 1647.
[2] M. Schubert, S. Hackenberg, A.C. van Veen, M. Muhler, V. Plzak, R.J. Behm, J. Catal. 197 (2001) 113.
[3] M. Haruta, T. Kobayashi, H. Sano, N. Yamada, Chem. Lett. 2 (1987) 405.
[4] B. Hammer, J.K. Nørskov, Nature 376 (1995) 238.
[5] J.B. Park, J. Graciano, J. Evans, D. Stacchiola, S.D. Senanayake, L. Barrio, P. Liu, J.F. Sanz, J. Hrbek, J.A. Rodriguez, J. Am. Chem. Soc. 132 (2010) 356.
[6] W.Y. Hernández, F. Romero-Sarria, M.A. Centeno, J.A. Odriozola, J. Phys. Chem. C 114 (2010) 10857.
[7] K.C. Taylor, Catal. Rev. Sci. Eng. 35 (1993) 457.
[8] N.W. Cant, P.W. Frederickson, J. Catal. 37 (1975) 531.
[9] A. Ueda, M. Haruta, Gold. Bull. 32 (1999) 3.
[10] J.R. Mellor, Catal. Today 72 (2002) 145.
[11] M. Comotti, W.-C. Li, B. Spliethoff, F. Schüth, J. Am. Chem. Soc. 128 (2006) 917.
[12] D.B. Akolekar, S.K. Bhargava, J. Mol. Catal. A: Chem. 236 (2005) 77.
[13] E.D.L. Rienks, G.P. van Berkel, J.W. Bakker, B.E. Nieuwenhuys, Surf. Sci. 571 (2004) 187.
[14] Catalysis by Gold G.C. Bond, C. Louis, D.T. Thompson (Eds.), Catalytic Science Series, vol. 6, Imperial College Press, London, 2006.
[15] C.P. Vinod, J.W. Niemantsverdriet, B.E. Niewenhuys, Appl. Catal. A: Gen. 291 (2005) 93–97.
[16] G. Ramis, G. Busca, V. Lorenzelli, P. Forzatti, Appl. Catal. A: Gen. 64 (1990) 243.
[17] K. Hadjiivanov, H. Knözinger, Phys. Chem. Chem. Phys. 2 (2000) 2803.
[18] J.C.S. Wu, Y.T. Chen, J. Catal. 237 (2006) 393.
[19] L. Li, Q. Shen, J. Chen, Z. Hao, Catal. Today 158 (2010) 361.
[20] M.A. Debeila, J. Phys. Chem. B 108 (2004) 18254.
[21] M.A. Debeila, N.J. Coville, M.S. Scurrell, G.R. Hearne, Catal. Today 72 (2002) 79.

[22] X. Deng, A. Verdaguer, T. Herranz, C. Weis, H. Bluhm, M. Salmeron, Langmuir 24 (2008) 9474.
[23] T. Herranz, X. Deng, A. Cabot, P.A. Alivisatos, Z. Liu, G. Soler-Illia, M. Salmeron, Catal. Today 143 (2009) 158.
[24] N.R. Jana, X. Peng, J. Am. Chem. Soc. 125 (2003) 14280.
[25] V.F. Puntes, D. Zanchet, C.K. Erdonmez, A.P. Alivisatos, J. Am. Chem. Soc. 124 (2002) 12874.
[26] A. Cabot, V.F. Puntes, E. Shevchenko, Y. Yin, L. Balcells, M.A. Marcus, S.M. Hughes, A. Alivisatos, J. Am. Chem. Soc. 129 (2007) 10358.
[27] J.R. Heath, C.M. Knobler, D.V. Leff, J. Phys. Chem. B 101 (1997) 189.
[28] R.M. Rioux, H. Song, M. Grass, S. Habas, K. Niesz, J.D. Hoefelmeyer, P. Yang, G.A. Somorjai, Top. Catal. 39 (2006) 167.
[29] E.L. Crepaldi, G.J.A.A. Soler-Illia, D. Grosso, F. Cagnol, F. Ribot, C. Sanchez, J. Am. Chem. Soc. 125 (2003) 9770.
[30] P.C. Angelome, L. Andrini, M.E. Calvo, F.G. Requejo, S.A. Bilmes, G.J.A.A. Soler-Illia, J. Phys. Chem. C 111 (2007) 10886.
[31] D.F. Ogletree, H. Bluhm, G. Lebedev, C.S. Fadley, Z. Hussain, M. Salmeron, Rev. Sci. Inst. 73 (2002) 3872.
[32] M. Salmeron, R. Schlögl, Surf. Sci. Rep. 63 (2008) 169.
[33] S. Porsgaard, P. Jiang, F. Borondics, S. Wendt, H. Bluhm, F. Besenbacher, M. Salmeron, Angew. Chem. Int. 123 (2011) 2314–2317.
[34] P. Jiang, S. Porsgaard, F. Borondics, M. Köber, A. Caballero, H. Bluhm, F. Besenbacher, M. Salmeron, J. Am. Chem. Soc. 132 (2010) 2858–2859.
[35] G. Ketteler, S. Yamamoto, H. Bluhm, K. Andersson, D.E. Starr, D.F. Ogletree, H. Ogasawara, A. Nilsson, M. Salmeron, J. Phys. Chem. C 11 (2007) 8278.
[36] J. Nowotny, T. Bak, L.R. Sheppard, M.K. Nowotny, J. Am. Chem. Soc. 130 (2008) 9984.
[37] J. Abad, O. Böhme, E. Roman, Langmuir 23 (2007) 7583.
[38] K. Hosaka, J. Adachi, M. Takahashi, A. Yagishita, J. Phys. B: At. Mol. Opt. Phys. 36 (2003) 4617–4629.
[40] J. Haubrich, R.G. Quiller, L. Benz, Z. Liu, C.M. Friend, Langmuir 26 (2010) 2445–2451.
[41] A.T.S. Wee, J. Lin, A.C.H. Huan, F.C. Loh, K.L. Tan, Surf. Sci. 304 (1994) 145.
[42] F. Nart, C. Friend, J. Phys. Chem. B 105 (2002) 2773–2778.
[43] Z. Shuxian, W.K. Hall, G. Ertl, H. Knozinger, J. Catal. 100 (1986) 167.

Further reading

[39] T. Shimada, B.S. Mun, I.F. Nakai, A. Banno, H. Abe, Y. Iwasawa, T. Ohta, H. Kondoh, J. Phys. Chem. C 114 (2010) 17030–17035.